

- [4] A. Scaglione, G. B. Giannakis, and S. Barbarossa, "Redundant filter bank precoders and equalizers—Part I: Unification and optimal designs," *IEEE Trans. Signal Process.*, vol. 47, no. 7, pp. 1988–2006, Jul. 1999.
- [5] A. Scaglione, G. B. Giannakis, and S. Barbarossa, "Redundant filter bank precoders and equalizers—Part II: Blind channel estimation, synchronization, and direct equalization," *IEEE Trans. Signal Process.*, vol. 47, no. 7, pp. 2007–2022, Jul. 1999.
- [6] Z. Wang, X. Ma, and G. B. Giannakis, "Optimality of single-carrier zero-padding block transmission," in *Proc. Wireless Communications Networking Conf.*, Mar. 2002, vol. 2, pp. 660–664.
- [7] Z. Wang and G. B. Giannakis, "Wireless multicarrier communications: Where Fourier meets Shannon," *IEEE Signal Process. Mag.*, vol. 17, no. 3, pp. 29–48, May 2000.
- [8] B. Muquet, Z. Wang, G. B. Giannakis, M. D. Courville, and P. Duhamel, "Cyclic prefixing or zero padding for wireless multicarrier transmissions?," *IEEE Trans. Commun.*, vol. 50, no. 12, pp. 2136–2148, Dec. 2002.
- [9] Z. Wang, X. Ma, and G. B. Giannakis, "OFDM or single-carrier block transmission?," *IEEE Trans. Commun.*, vol. 52, no. 3, pp. 380–394, Mar. 2004.
- [10] S. Zhou and G. B. Giannakis, "Finite-alphabet based channel estimation for OFDM and related multicarrier systems," *IEEE Trans. Commun.*, vol. 49, no. 8, pp. 1402–1414, Mar. 2001.
- [11] X. Ma, G. B. Giannakis, and S. Barbarossa, "Non-data-aided frequency-offset and channel estimation in OFDM and related block transmissions," in *Proc. IEEE Int. Conf. Communications*, Jun. 2001, vol. 6, pp. 1866–1870.
- [12] X. G. Doukopoulos and G. V. Moustakides, "Adaptive algorithms for blind channel estimation in OFDM systems," in *Proc. IEEE Int. Conf. Communications*, Jun. 2004, vol. 4, pp. 2377–2381.
- [13] Y. H. Zeng and T. S. Ng, "A semi-blind channel estimation method for multiuser multiantenna OFDM systems," *IEEE Trans. Signal Process.*, vol. 52, no. 5, pp. 1419–1429, May 2004.
- [14] H. Bölcskei, R. W. Heath, Jr., and A. J. Paulraj, "Blind channel identification and equalization in OFDM-based multiantenna systems," *IEEE Trans. Signal Process.*, vol. 50, no. 1, pp. 96–109, Jan. 2002.
- [15] Z. Ding and L. Qiu, "Blind MIMO channel identification from second order statistics using rank deficient channel convolution matrix," *IEEE Trans. Signal Process.*, vol. 51, no. 2, pp. 535–544, Feb. 2003.
- [16] K. Abed-Meraim, W. Qiu, and Y. Hua, "Blind system identification," *Proc. IEEE*, vol. 85, no. 8, pp. 1310–1332, Aug. 1997.
- [17] Z. Ding and Y. Li, *Blind Equalization and Identification*. New York: Marcel Dekker, 2001.
- [18] G. B. Giannakis, Y. Hua, P. Stoica, and L. Tong, *Signal Processing Advances in Wireless and Mobile Communications Volume I: Trends in Channel Identification and Equalization*. Englewood Cliffs, NJ: Prentice-Hall PTR, 2001.

## Quasi-Orthogonal Time-Reversal Space-Time Block Coding for Frequency-Selective Fading Channels

Hakam Mheidat, *Student Member, IEEE*,  
Murat Uysal, *Member, IEEE*, and  
Naofal Al-Dhahir, *Senior Member, IEEE*

**Abstract**—Quasi-orthogonal space-time block codes (QO-STBCs) are a powerful code family designed for more than two transmit antennas. In contrast to their orthogonal counterparts designed for the same number of transmit antennas, QO-STBCs are able to provide full-rate transmission rate. While original QO-STBCs enjoy only a partial diversity, the recently proposed rotated versions of QO-STBCs achieve the maximum diversity order which is equal to the number of transmit antennas. Since QO-STBCs have been originally proposed for frequency-flat fading channels, it is a challenging design problem to apply them over frequency-selective channels. The dispersive nature of such channels results in intersymbol interference which needs to be carefully handled at the receiver. In this paper, we investigate time-domain equalization for QO-STBC, exploiting the embedded quasi-orthogonal structure to design low-complexity receivers. We also present diversity gains for the proposed scheme through pairwise error probability (PEP) derivation and analysis which are further confirmed by Monte Carlo simulations.

**Index Terms**—Cooperative diversity, distributed space-time block coding, equalization, fading channels, pairwise error probability.

### I. INTRODUCTION

Space-time trellis codes (STTCs) introduced in [1] are an effective transmit diversity technique to combat fading effects in wireless communication systems. STTCs are designed to achieve maximum diversity gain; however, for a fixed number of transmit antennas, their decoding complexity increases exponentially with the transmission rate. Space-time block codes (STBCs) [2], [3] were proposed as an attractive alternative to their trellis counterparts with a much lower decoding complexity due to their inherent orthogonal structure. In STBCs, the received signals are decoupled after spatio-temporal matched filtering; hence, the complexity increases only linearly with the codeword size. However, these codes suffer a loss in throughput efficiency for more than two transmit antennas. The STBC designed for two transmit antennas, i.e., Alamouti's scheme [3], is able to achieve the full diversity and full transmission rate for both real and complex signal constellations. The other STBCs proposed in [2] for more antennas enjoy the full diversity at full transmission rate only for real signal constellations. It is further proven in [4], [5] that the rates cannot be greater than 3/4 for more than two antennas with complex signal constellation under the orthogonality assumption.

Manuscript received September 4, 2005; revised January 31, 2006. The associate editor coordinating the review of this manuscript and approving it for publication was Prof. Javier Garcia-Frias. This paper was presented in part at IEEE International Conference on Communications (ICC), Paris, France, June 2004. The work of M. Uysal is supported in part by an NSERC Special Opportunity Grant (SROPJ305821-05). The work of N. Al-Dhahir is supported in part by the Texas Advanced Technology (ATP) program contract no. 009741-0023-2003 and by NSF contracts CCF 0430654 and DMS 0528010.

H. Mheidat and M. Uysal are with the Department of Electrical and Computer Engineering, University of Waterloo, ON N2G3L1, Canada (e-mail: hmheidat@ece.uwaterloo.ca; muysal@ece.uwaterloo.ca).

N. Al-Dhahir is with the Department of Electrical Engineering, The University of Texas at Dallas, Richardson, TX 75083-0688 USA (e-mail: aldhahir@utdallas.edu).

Digital Object Identifier 10.1109/TSP.2006.885766

To address transmission rate efficiency, Jafarkhani [6], Papadias and Foschini [7], and Tirkkonen *et al.* [8] independently proposed so-called quasi-orthogonal STBCs (QO-STBCs) for four transmit antennas,<sup>1</sup> where the orthogonality assumption is relaxed to achieve full transmission rate  $R = 1$ . QO-STBCs allow so-called “pair-decoding”<sup>2</sup> [6], [8] and allow a relatively low-complexity receiver implementation where the decoding complexity grows proportionally with  $M^2$  with  $M$  as the constellation size. However, these codes only provide a partial diversity of 2. Recently, rotated QO-STBCs (R-QO-STBCs) have been proposed in [9]–[11], which give full diversity at full transmission rate while still keeping the same decoding complexity of their original counterparts. R-QO-STBCs are based on the original QO-STBCs, where half of the symbols in the original codes are chosen from a given signal constellation set while the other half is chosen from a phase-rotated version of the same constellation. Carefully optimized rotation angles yield codes with full diversity.

Since QO-STBCs (both original and rotated versions) have been proposed for frequency-flat fading channels, it is challenging to apply them over frequency-selective channels. The dispersive nature of such channels results in intersymbol interference (ISI), leading to an inevitable performance degradation. Various equalization techniques, which were originally developed for single-input single-output (SISO) antenna systems can be extended for space-time coded systems. A comprehensive review of equalization techniques for multiple antenna systems can be found in [12]. Among the proposed equalization methods for STBC, time-reversal (TR) equalization [13] deserves particular attention due to its ability to exploit the orthogonal structure over frequency-selective channels. Inspired from [13], we investigate TR equalization for QO-STBC in the current paper carefully exploiting the inherent quasi-orthogonality. To the best of our knowledge, the conference version of this paper [14] is the first attempt to extend QO-STBCs for frequency-selective fading channels. The proposed scheme is essentially an extension of the QO-STBCs to frequency-selective channels by imposing the quasi-orthogonal structure at a block-level instead of the symbol-level realization for the flat-fading channel case. Our performance analysis through pairwise error probability (PEP) derivation reveals that the proposed scheme is able to exploit fully both spatial and multipath diversity when R-QO-STBCs are considered. We also demonstrate that our proposed block-level implementation allows pair decoupling over frequency-selective channels similar to its symbol-level counterpart designed for frequency-flat channels. Although the resulting complexity is practically feasible for most scenarios, pair-decoding complexity might be still prohibitive for higher-order modulation schemes and long channel memories. Thus, we further consider alternative QO-STBCs which allow “full decoupling” (in contrast to pair decoupling) and, therefore, bring a significant complexity reduction in the receiver design. Although they are able to exploit only partial diversity, their performance in practical signal-to-noise ratio (SNR) range is comparable to full-diversity QO-STBCs and, thus, provide an attractive alternative to them.

The rest of the paper is organized as follows: In Section II, the transmission model is introduced. In Section III, we present the respective PEP derivation and the diversity gain analysis. QO-STBCs, which allow full decoupling, are studied in Section IV. Numerical results are presented in Section V, and the paper is concluded in Section VI.

*Notation:*  $(\cdot)^*$ ,  $(\cdot)^T$ , and  $(\cdot)^H$  denote conjugate, transpose, and Hermitian transpose operations, respectively.  $\otimes$  denotes convolution,  $E[\cdot]$  denotes expectation,  $[\cdot]_{k,l}$  denotes the  $(k,l)$ th entry of a matrix,

<sup>1</sup>These codes can be generalized for  $2^n$  ( $n > 2$ ) transmit antennas.

<sup>2</sup>This property of QO-STBC is sometimes referred to as “pair-decoupling” in this paper.

$[\cdot]_k$  denotes the  $k$ th entry of a vector and  $\|\cdot\|$  denotes the Euclidean norm of a vector,  $\mathbf{I}_M$  denotes the identity matrix of size  $M \times M$ ,  $\mathbf{1}_{M \times M}$  denotes all-ones matrix of size  $M \times M$ , and  $\mathbf{0}_{M \times M}$  denotes all-zero matrix of size  $M \times M$ . Bold upper-case letters denote matrices and bold lower-case letters denote vectors.

## II. TRANSMISSION MODEL

We consider space-time block transmission assuming a single receive antenna and four transmit antennas over a frequency-selective fading wireless channel although our approach can be extended to multiple receive antennas and  $2^n$  ( $n > 2$ ) transmit antennas in a straightforward manner. Specifically, we focus on the QO-STBC proposed by Tirkkonen *et al.* [8], noting that the discussion for the Jafarkhani scheme [6] and the Papadias–Foschini scheme [7] is similar. The QO-STBC transmission matrix is built from two Alamouti codes. Defining the underlying Alamouti codes as

$$\mathbf{A}_{12} = \begin{bmatrix} x_1 & x_2 \\ -x_2^* & x_1^* \end{bmatrix}, \quad \mathbf{A}_{34} = \begin{bmatrix} x_3 & x_4 \\ -x_4^* & x_3^* \end{bmatrix}$$

the resulting QO-STBC code is given by the following  $4 \times 4$  matrix [8]

$$\mathbf{A} = \begin{bmatrix} \mathbf{A}_{12} & \mathbf{A}_{34} \\ \mathbf{A}_{34} & \mathbf{A}_{12} \end{bmatrix} = \begin{pmatrix} x_1 & x_2 & x_3 & x_4 \\ -x_2^* & x_1^* & -x_4^* & x_3^* \\ x_3 & x_4 & x_1 & x_2 \\ -x_4^* & x_3^* & -x_2^* & x_1^* \end{pmatrix}. \quad (1)$$

This code provides full rate transmission rate and achieves a diversity order of 2 over frequency-flat channels. Here, we apply the idea of time-reversal equalization originally proposed for Alamouti STBC scheme [3] to the quasi-orthogonal code in (1), exploiting the embedded quasi-orthogonal structure to decouple the input streams (in pairs). Information symbols are first parsed to four streams of  $M \times 1$  blocks  $\mathbf{x}_i$ ,  $i = 1, 2, 3, 4$ <sup>3</sup> and then multiplied by a zero-padding (ZP) matrix  $\Psi = [\mathbf{I}_M^T, \mathbf{0}_{M \times L}^T]^T$  of size  $N \times M$ , where  $N$  is the frame length. To further remove interblock interference and make the channel matrix circulant, a cyclic prefix (CP) of length  $L$  is added between adjacent information blocks. Due to the adopted precoding form, i.e., zero padding, we simply insert additional zeros at the start of the frame as CP. In practical implementation, the block of all zeros at the end of the current frame can also be used as the next frame’s block of all zeros to be inserted at its beginning, avoiding unnecessary additional overhead.

Based on (1), the following encoding rule is implemented which will allow decoupling (in pairs) at the receiver side ( $k = 0, 4, 8, \dots$ ) (cf. Fig. 1):

$$\begin{aligned} \mathbf{d}_{1,k+1} &= -\mathbf{J}\mathbf{d}_{2,k}^*, & \mathbf{d}_{2,k+1} &= \mathbf{J}\mathbf{d}_{1,k}^* \\ \mathbf{d}_{1,k+2} &= \mathbf{d}_{3,k}, & \mathbf{d}_{2,k+2} &= \mathbf{d}_{4,k} \\ \mathbf{d}_{1,k+3} &= -\mathbf{J}\mathbf{d}_{4,k}^*, & \mathbf{d}_{2,k+3} &= \mathbf{J}\mathbf{d}_{3,k}^* \\ \mathbf{d}_{3,k+1} &= -\mathbf{J}\mathbf{d}_{4,k}^*, & \mathbf{d}_{4,k+1} &= \mathbf{J}\mathbf{d}_{3,k}^* \\ \mathbf{d}_{3,k+2} &= \mathbf{d}_{1,k}, & \mathbf{d}_{4,k+2} &= \mathbf{d}_{4,k} \\ \mathbf{d}_{3,k+3} &= -\mathbf{J}\mathbf{d}_{2,k}^*, & \mathbf{d}_{4,k+3} &= \mathbf{J}\mathbf{d}_{1,k}^* \end{aligned}$$

where  $\mathbf{d}_i = \Psi \mathbf{x}_i$  is the zero-padded information vector and  $\mathbf{J}$  is a partial permutation matrix<sup>4</sup> [15].

<sup>3</sup>Any linear modulation technique such as QAM or PSK modulation can be used.

<sup>4</sup>For  $\mathbf{a} = [\mathbf{a}(0), \dots, \mathbf{a}(M+L-1)]$ ,  $\mathbf{a} = [\mathbf{a}(M-1), \dots, \mathbf{a}(0), \mathbf{a}(M+L-1), \dots, \mathbf{a}(M)]$ .

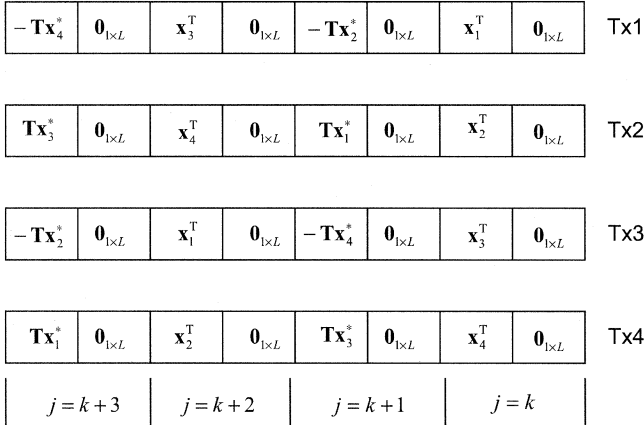


Fig. 1. Transmission format for TR-QO-STBC.  $\mathbf{T}$  denotes the  $M \times M$  time-reversal matrix which consists of ones on the main anti-diagonal and zeros elsewhere.

We consider a frequency-selective channel where the channel impulse response (CIR) from the  $i$ th ( $i = 1, 2, 3, 4$ ) transmit antenna to the receive antenna at block  $j$  ( $j = k + 1, k + 2, k + 3, k + 4$ ) is modeled as a finite-impulse-response (FIR) filter with memory  $L$  and denoted by  $\mathbf{h}_{i,j} = [\mathbf{h}_{i,j}(0) \ \mathbf{h}_{i,j}(1) \ \dots \ \mathbf{h}_{i,j}(L)]^T$ . The entries of the random vectors  $\mathbf{h}_{i,j}$  are assumed to be independent and identically distributed zero-mean complex Gaussian with power delay profile vector denoted by  $\mathbf{v} = [\sigma^2(0), \dots, \sigma^2(L)]$  and are normalized such that  $\sum_{l=0}^L \sigma^2(l) = 1$ . The CIRs are assumed to be constant over four consecutive blocks and vary independently every four blocks. The signal received at the receiver is given as

$$\mathbf{r}_j = \sum_{i=1}^4 \mathbf{H}_{i,j} \Psi \mathbf{x}_{i,j} + \mathbf{n}_j \quad (2)$$

where  $\mathbf{H}_{i,j}$  ( $i = 1, 2, 3, 4$ ) is an  $N \times N$  circulant matrix with entries  $[\mathbf{H}_{i,j}]_{k,l} = \mathbf{h}_{i,j}((k-l) \bmod N)$  and  $\mathbf{n}_j$  is the additive white Gaussian noise vector with each entry having zero mean and variance of  $N_0/2$  per dimension. Assuming that the channel coefficients remain constant over blocks  $k, k+1, k+2$ , and  $k+3$ , i.e.,  $\mathbf{H}_{i,k} = \mathbf{H}_{i,k+1} = \mathbf{H}_{i,k+2} = \mathbf{H}_{i,k+3} = \mathbf{H}_i$ ,  $i = 1, 2, 3, 4$ , the received signals can be written in a matrix form as

$$\underbrace{\begin{bmatrix} \mathbf{r}_k \\ \tilde{\mathbf{r}}_{k+1} \\ \mathbf{r}_{k+2} \\ \tilde{\mathbf{r}}_{k+3} \end{bmatrix}}_{\mathbf{r}} = \underbrace{\begin{bmatrix} \mathbf{H}_1 & \mathbf{H}_2 & \mathbf{H}_3 & \mathbf{H}_4 \\ \mathbf{H}_2^H & -\mathbf{H}_1^H & \mathbf{H}_4^H & -\mathbf{H}_3^H \\ \mathbf{H}_3 & \mathbf{H}_4 & \mathbf{H}_1 & \mathbf{H}_2 \\ \mathbf{H}_4^H & -\mathbf{H}_3^H & \mathbf{H}_2^H & -\mathbf{H}_1^H \end{bmatrix}}_{\mathbf{H}} \underbrace{\begin{bmatrix} \mathbf{d}_{1,k} \\ \mathbf{d}_{2,k} \\ \mathbf{d}_{3,k} \\ \mathbf{d}_{4,k} \end{bmatrix}}_{\mathbf{d}} + \underbrace{\begin{bmatrix} \mathbf{n}_k \\ \mathbf{J}\mathbf{n}_{k+1} \\ \mathbf{n}_{k+2} \\ \mathbf{J}\mathbf{n}_{k+3} \end{bmatrix}}_{\mathbf{n}} \quad (3)$$

where we define  $\tilde{\mathbf{r}}_{k+1} = \mathbf{J}\mathbf{r}_{k+1}^*$  and  $\tilde{\mathbf{r}}_{k+3} = \mathbf{J}\mathbf{r}_{k+3}^*$ . Equivalently, (3) can be rewritten as (4), shown at the bottom of the page. Let  $M$  denote

$$\mathbf{M} = \begin{bmatrix} (\mathbf{H}_a)^{-1/2} & \mathbf{0}_N & \mathbf{0}_N & \mathbf{0}_N \\ \mathbf{0}_N & (\mathbf{H}_a)^{-1/2} & \mathbf{0}_N & \mathbf{0}_N \\ \mathbf{0}_N & \mathbf{0}_N & (\mathbf{H}_b)^{-1/2} & \mathbf{0}_N \\ \mathbf{0}_N & \mathbf{0}_N & \mathbf{0}_N & (\mathbf{H}_b)^{-1/2} \end{bmatrix}$$

where we define  $\mathbf{H}_a = |\mathbf{H}_1 + \mathbf{H}_3|^2 + |\mathbf{H}_2 + \mathbf{H}_4|^2$  and  $\mathbf{H}_b = |\mathbf{H}_1 - \mathbf{H}_3|^2 + |\mathbf{H}_2 - \mathbf{H}_4|^2$ . Multiplying (4) by  $\mathbf{M}\mathbf{H}_{\text{eqv}}^H$ , i.e., spatio-temporal filtering, we decouple the output of spatio-temporal filter into four streams as follows:

$$\mathbf{r}_{\text{out},k} = \mathbf{H}_a^{1/2} (\mathbf{d}_{1,k} + \mathbf{d}_{3,k}) + \mathbf{n}_{\text{out},k} \quad (5)$$

$$\mathbf{r}_{\text{out},k+1} = \mathbf{H}_a^{1/2} (\mathbf{d}_{2,k} + \mathbf{d}_{4,k}) + \mathbf{n}_{\text{out},k+1} \quad (6)$$

$$\mathbf{r}_{\text{out},k+2} = \mathbf{H}_b^{1/2} (\mathbf{d}_{1,k} - \mathbf{d}_{3,k}) + \mathbf{n}_{\text{out},k+2} \quad (7)$$

$$\mathbf{r}_{\text{out},k+3} = \mathbf{H}_b^{1/2} (\mathbf{d}_{2,k} - \mathbf{d}_{4,k}) + \mathbf{n}_{\text{out},k+3} \quad (8)$$

where  $\mathbf{n}_{\text{out},j}$  represents the filtered noise vector which is still Gaussian with each entry having zero mean and a variance of  $N_0$  per dimension. It should be noted that in (5) and (8), a pair of data vectors is embedded in each of the streams. This can be defined as ‘‘pair decoupling’’ (in contrast to full decoupling associated with orthogonal STBC) and requires so-called ‘‘pair decoding’’ [6]. The resulting data streams can be now detected by applying standard equalization techniques such as maximum-likelihood sequence estimation (MLSE) [16] or minimum mean-square error (MMSE) equalizers [17, pp. 68–69, 147]. For MLSE implementation, the ML detection of the transmitted symbols amounts to minimizing the following metrics:

$$\begin{aligned} (\hat{\mathbf{d}}_{1,k}, \hat{\mathbf{d}}_{3,k}) = \arg \min_{(\mathbf{d}_{1,k}, \mathbf{d}_{3,k})} & \left\{ \left\| \mathbf{r}_{\text{out},k} - \mathbf{H}_a^{1/2} (\mathbf{d}_{1,k} + \mathbf{d}_{3,k}) \right\|^2 \right. \\ & \left. + \left\| \mathbf{r}_{\text{out},k+2} - \mathbf{H}_b^{1/2} (\mathbf{d}_{1,k} - \mathbf{d}_{3,k}) \right\|^2 \right\} \quad (9) \end{aligned}$$

$$\begin{aligned} (\hat{\mathbf{d}}_{2,k}, \hat{\mathbf{d}}_{4,k}) = \arg \min_{(\mathbf{d}_{2,k}, \mathbf{d}_{4,k})} & \left\{ \left\| \mathbf{r}_{\text{out},k+1} - \mathbf{H}_a^{1/2} (\mathbf{d}_{2,k} + \mathbf{d}_{4,k}) \right\|^2 \right. \\ & \left. + \left\| \mathbf{r}_{\text{out},k+3} - \mathbf{H}_b^{1/2} (\mathbf{d}_{2,k} - \mathbf{d}_{4,k}) \right\|^2 \right\}. \quad (10) \end{aligned}$$

The total number of states in the trellis implementation is  $M^{2(L+1)}$  (where  $M$  is the constellation size) which exhibits a complexity reduction by a factor of  $M^{2(L+1)}$  compared with a ‘‘full’’ MLSE equalizer design with  $M^{4(L+1)}$  states for four transmit antennas. Even this decreased complexity might still be computationally intensive for certain

$$\begin{bmatrix} \mathbf{r}_k \\ \tilde{\mathbf{r}}_{k+1} \\ \mathbf{r}_{k+2} \\ \tilde{\mathbf{r}}_{k+3} \end{bmatrix} = \frac{1}{2} \underbrace{\begin{bmatrix} \mathbf{H}_1 + \mathbf{H}_3 & \mathbf{H}_2 + \mathbf{H}_4 & \mathbf{H}_1 - \mathbf{H}_3 & \mathbf{H}_2 - \mathbf{H}_4 \\ \mathbf{H}_2^H + \mathbf{H}_4^H & -(\mathbf{H}_1^H + \mathbf{H}_3^H) & \mathbf{H}_2^H - \mathbf{H}_4^H & -(\mathbf{H}_1^H - \mathbf{H}_3^H) \\ \mathbf{H}_1 + \mathbf{H}_3 & \mathbf{H}_2 + \mathbf{H}_4 & -(\mathbf{H}_1 - \mathbf{H}_3) & -(\mathbf{H}_2 - \mathbf{H}_4) \\ \mathbf{H}_2^H + \mathbf{H}_4^H & -(\mathbf{H}_1^H + \mathbf{H}_3^H) & -(\mathbf{H}_2^H - \mathbf{H}_4^H) & \mathbf{H}_1^H - \mathbf{H}_3^H \end{bmatrix}}_{\mathbf{H}_{\text{eqv}}} \begin{bmatrix} \mathbf{d}_{1,k} + \mathbf{d}_{3,k} \\ \mathbf{d}_{2,k} + \mathbf{d}_{4,k} \\ \mathbf{d}_{1,k} - \mathbf{d}_{3,k} \\ \mathbf{d}_{2,k} - \mathbf{d}_{4,k} \end{bmatrix} + \begin{bmatrix} \mathbf{n}_k \\ \mathbf{J}\mathbf{n}_{k+1} \\ \mathbf{n}_{k+2} \\ \mathbf{J}\mathbf{n}_{k+3} \end{bmatrix}. \quad (4)$$

scenarios with higher order modulations and long channel memory. A suboptimal but lower complexity MMSE equalizer provides an attractive alternative [17, pp. 68–69, 147]. For the MMSE equalizer, the outputs of the MMSE filter are given by

$$\mathbf{r}_{\text{filter},j} = \begin{cases} \boldsymbol{\xi}_a \otimes \hat{\mathbf{r}}_{\text{out},j}, & j = k, k+1 \\ \boldsymbol{\xi}_b \otimes \hat{\mathbf{r}}_{\text{out},j}, & j = k+2, k+3 \end{cases} \quad (11)$$

where  $\boldsymbol{\xi}_a = (\boldsymbol{\Gamma}_1^H \boldsymbol{\Gamma}_1 + \boldsymbol{\Gamma}_1 / \text{SNR}) \boldsymbol{\Gamma}_1^H \mathbf{e}_0$  and  $\boldsymbol{\xi}_b = (\boldsymbol{\Gamma}_2^H \boldsymbol{\Gamma}_2 + \boldsymbol{\Gamma}_2 / \text{SNR})^{-1} \boldsymbol{\Gamma}_2^H \mathbf{e}_0$  are the filter coefficients of length  $2F+1$  ( $2F > L$ ). Here,  $\mathbf{e}_0$  is a  $(2F+1)$  vector whose  $(F+1)$ th element is equal to one and other elements are zeros,  $\boldsymbol{\Gamma}_1$  and  $\boldsymbol{\Gamma}_2$  are  $(2F+1) \times (2F+1)$  Toeplitz matrixes [17] with entries equal to the nonzero elements in the first columns of  $\mathbf{H}_a^{1/2}$  and  $\mathbf{H}_b^{1/2}$ , respectively, and SNR represents the signal-to-noise-ratio. The signals in (11) are then fed into a minimum Euclidean distance decoder to recover the transmitted symbols.

### III. DIVERSITY GAIN ANALYSIS

In this section, we examine the maximum achievable diversity gain for TR-QO-STBC through the derivation of PEP expression. We will start by dropping the block index  $j = k, k+1, k+2, k+3$  for notational brevity. The transmitted codeword vector and the erroneously decoded codeword sequence are denoted as  $(\mathbf{x}_1, \mathbf{x}_3, \mathbf{x}_2, \mathbf{x}_4)$  and  $(\hat{\mathbf{x}}_1, \hat{\mathbf{x}}_3, \hat{\mathbf{x}}_2, \hat{\mathbf{x}}_4)$ , respectively. However, due to the symmetry of problem at hand, we consider only the pair  $(\mathbf{x}_1, \mathbf{x}_3)$  and its erroneously decoded version  $(\hat{\mathbf{x}}_1, \hat{\mathbf{x}}_3)$ . Thus, a Chernoff bound on the conditional PEP is given by

$$P((\mathbf{x}_1, \mathbf{x}_3), (\hat{\mathbf{x}}_1, \hat{\mathbf{x}}_3) | \mathbf{H}_1, \mathbf{H}_2, \mathbf{H}_3, \mathbf{H}_4) \leq \exp\left(-\frac{d^2((\mathbf{x}_1, \mathbf{x}_3), (\hat{\mathbf{x}}_1, \hat{\mathbf{x}}_3))}{8N_0}\right) \quad (12)$$

assuming MLSE decoding with perfect knowledge of the channel state information (CSI) at the receiver side. Here,  $d^2((\mathbf{x}_1, \mathbf{x}_3), (\hat{\mathbf{x}}_1, \hat{\mathbf{x}}_3))$  denotes the Euclidean distance between  $(\mathbf{x}_1, \mathbf{x}_3)$  and  $(\hat{\mathbf{x}}_1, \hat{\mathbf{x}}_3)$ . Noting that  $\mathbf{d}_i = \boldsymbol{\Psi}_i \mathbf{x}_i$  and defining  $\mathbf{e}_1 = \mathbf{d}_1 - \hat{\mathbf{d}}_1$ ,  $\mathbf{e}_3 = \mathbf{d}_3 - \hat{\mathbf{d}}_3$ , we have

$$d^2((\mathbf{x}_1, \mathbf{x}_3), (\hat{\mathbf{x}}_1, \hat{\mathbf{x}}_3)) = \|(\mathbf{H}_1 + \mathbf{H}_3)(\mathbf{e}_1 + \mathbf{e}_3)\|^2 + \|(\mathbf{H}_2 + \mathbf{H}_4)(\mathbf{e}_1 + \mathbf{e}_3)\|^2 + \|(\mathbf{H}_1 - \mathbf{H}_3)(\mathbf{e}_1 - \mathbf{e}_3)\|^2 + \|(\mathbf{H}_2 - \mathbf{H}_4)(\mathbf{e}_1 - \mathbf{e}_3)\|^2. \quad (13)$$

Introducing (14), shown at the bottom of the page, we can rewrite (13) as

$$d^2((\mathbf{x}_1, \mathbf{x}_3), (\hat{\mathbf{x}}_1, \hat{\mathbf{x}}_3)) = \left\| (\mathbf{h}_1 + \mathbf{h}_3)^T (\mathbf{E}_1 + \mathbf{E}_3) \right\|^2 + \left\| (\mathbf{h}_2 + \mathbf{h}_4)^T (\mathbf{E}_1 + \mathbf{E}_3) \right\|^2 + \left\| (\mathbf{h}_1 - \mathbf{h}_3)^T (\mathbf{E}_1 - \mathbf{E}_3) \right\|^2 + \left\| (\mathbf{h}_2 - \mathbf{h}_4)^T (\mathbf{E}_1 - \mathbf{E}_3) \right\|^2 \quad (15)$$

which has the desired form for the rest of derivation. The main idea besides the rotated QO-STBC is to exploit signal constellation phase rotations to achieve full diversity [9]–[11]. For instance, if  $\mathbf{d}_1$  belongs to the signal constellation set  $\vartheta$ , then it must be ensured that  $\mathbf{d}_3$  belongs to the rotated constellation set  $e^{j\theta}\vartheta$ , so that  $\mathbf{E}_1$  and  $\mathbf{E}_3$  in (15) would belong to different constellations. Defining  $\boldsymbol{\eta}_1^T = (\mathbf{h}_1 + \mathbf{h}_3)^T$ ,  $\boldsymbol{\eta}_2^T = (\mathbf{h}_2 + \mathbf{h}_4)^T$ ,  $\boldsymbol{\eta}_3^T = (\mathbf{h}_1 - \mathbf{h}_3)^T$ , and  $\boldsymbol{\eta}_4^T = (\mathbf{h}_2 - \mathbf{h}_4)^T$ , where the entries of  $\boldsymbol{\eta}_i$ ,  $i = 1, 2, 3, 4$ , are independent zero-mean complex Gaussian with power delay profile vector  $\tilde{\mathbf{v}} = [2\sigma^2(0), \dots, 2\sigma^2(L)]$ , we can write (15) as

$$d^2((\mathbf{x}_1, \mathbf{x}_3), (\hat{\mathbf{x}}_1, \hat{\mathbf{x}}_3)) = \boldsymbol{\eta}_1^T \boldsymbol{\chi}_1 \left( \boldsymbol{\eta}_1^T \right)^H + \boldsymbol{\eta}_2^T \boldsymbol{\chi}_1 \left( \boldsymbol{\eta}_2^T \right)^H + \boldsymbol{\eta}_3^T \boldsymbol{\chi}_2 \left( \boldsymbol{\eta}_3^T \right)^H + \boldsymbol{\eta}_4^T \boldsymbol{\chi}_2 \left( \boldsymbol{\eta}_4^T \right)^H \quad (16)$$

where  $\boldsymbol{\chi}_1 = (\mathbf{E}_1 + \mathbf{E}_3)(\mathbf{E}_1 + \mathbf{E}_3)^H$  and  $\boldsymbol{\chi}_2 = (\mathbf{E}_1 - \mathbf{E}_3)(\mathbf{E}_1 - \mathbf{E}_3)^H$ . Introducing  $\boldsymbol{\mu}_i = \boldsymbol{\Omega}^{-1/2} \boldsymbol{\eta}_i$  where  $\boldsymbol{\Omega} = \text{diag}(\tilde{\mathbf{v}})$ , we can easily verify that the entries of  $\boldsymbol{\mu}_i$  have unit variance. Since  $\boldsymbol{\eta}_i$  and  $\boldsymbol{\Omega}^{1/2} \boldsymbol{\mu}_i$  have identical distributions, i.e., zero-mean, complex Gaussian with independent and identically distributed (i.i.d.) entries, we can rewrite (16) as

$$d^2((\mathbf{x}_1, \mathbf{x}_3), (\hat{\mathbf{x}}_1, \hat{\mathbf{x}}_3)) = \boldsymbol{\mu}_1^T \boldsymbol{\Omega}^{1/2} \boldsymbol{\chi}_1 \boldsymbol{\Omega}^{1/2} \left( \boldsymbol{\mu}_1^T \right)^H + \boldsymbol{\mu}_2^T \boldsymbol{\Omega}^{1/2} \boldsymbol{\chi}_1 \boldsymbol{\Omega}^{1/2} \left( \boldsymbol{\mu}_2^T \right)^H + \boldsymbol{\mu}_3^T \boldsymbol{\Omega}^{1/2} \boldsymbol{\chi}_2 \boldsymbol{\Omega}^{1/2} \left( \boldsymbol{\mu}_3^T \right)^H + \boldsymbol{\mu}_4^T \boldsymbol{\Omega}^{1/2} \boldsymbol{\chi}_2 \boldsymbol{\Omega}^{1/2} \left( \boldsymbol{\mu}_4^T \right)^H \quad (17)$$

Since  $\boldsymbol{\Omega}^{1/2} \boldsymbol{\chi}_i \boldsymbol{\Omega}^{1/2}$  is a  $(L+1) \times (L+1)$  Hermitian matrix, there exists a unitary matrix  $\mathbf{U}_i$  such that  $\mathbf{U}_i^H \boldsymbol{\Omega}^{1/2} \boldsymbol{\chi}_i \boldsymbol{\Omega}^{1/2} \mathbf{U}_i = \boldsymbol{\Delta}_i$  where  $\boldsymbol{\Delta}_i$  is a real diagonal matrix of size  $(L+1) \times (L+1)$  with non-negative

$$\mathbf{E}_i = \begin{bmatrix} [\mathbf{d}_i]_0 - [\hat{\mathbf{d}}_i]_0 & [\mathbf{d}_i]_1 - [\hat{\mathbf{d}}_i]_1 & \dots & [\mathbf{d}_i]_{N-1} - [\hat{\mathbf{d}}_i]_{N-1} \\ [\mathbf{d}_i]_{N-1} - [\hat{\mathbf{d}}_i]_{N-1} & [\mathbf{d}_i]_0 - [\hat{\mathbf{d}}_i]_0 & \dots & [\mathbf{d}_i]_{N-2} - [\hat{\mathbf{d}}_i]_{N-2} \\ \vdots & \vdots & \dots & \vdots \\ [\mathbf{d}_i]_{N-L} - [\hat{\mathbf{d}}_i]_{N-L} & [\mathbf{d}_i]_{N-L+1} - [\hat{\mathbf{d}}_i]_{N-L+1} & \dots & [\mathbf{d}_i]_{N-L-1} - [\hat{\mathbf{d}}_i]_{N-L-1} \end{bmatrix} \quad (14)$$

entries. Noting that the diagonal elements of  $\Delta_i$  are the eigenvalues of  $\mathbf{x}_i$ , (17) yields

$$\begin{aligned} d^2((\mathbf{x}_1, \mathbf{x}_3), (\hat{\mathbf{x}}_1, \hat{\mathbf{x}}_3)) &= \sum_{l=0}^L |\beta_1(l)|^2 \lambda_1(l) \\ &+ \sum_{l=0}^L |\beta_2(l)|^2 \lambda_1(l) \\ &+ \sum_{l=0}^L |\beta_3(l)|^2 \lambda_2(l) \\ &+ \sum_{l=0}^L |\beta_4(l)|^2 \lambda_2(l) \end{aligned} \quad (18)$$

where  $\beta_i = \boldsymbol{\mu}_i^T \mathbf{U}_j$  ( $i = 1, 2$  for  $j = 1$  and  $i = 3, 4$  for  $j = 2$ ), and  $\lambda_i(l)$  denotes the  $l$ th eigenvalue of  $\Delta_i$  ( $i = 1, 2$ ). Substituting (18) in (12), averaging the resulting expression with respect to the Rayleigh random variables  $|\beta_i(l)|$ ,  $i = 1, 2, 3, 4$  and assuming high SNR, we can obtain the final PEP expression as

$$\begin{aligned} P((\mathbf{x}_1, \mathbf{x}_3), (\hat{\mathbf{x}}_1, \hat{\mathbf{x}}_3)) &\leq \left(\frac{1}{8N_0}\right)^{-4(L+1)} \\ &\times \left(\prod_{l=0}^L \lambda_1(l)\right)^{-2} \left(\prod_{l=0}^L \lambda_2(l)\right)^{-2}. \end{aligned} \quad (19)$$

It is observed from (19) that the rotated QO-TR-STBC is able to achieve a diversity order of  $4(L+1)$ . If rotation is not considered as in the original schemes of [6]–[8], the resulting QO-STBC cannot guarantee full diversity. For example, if the transmitted symbols  $\mathbf{d}_1$  and  $\mathbf{d}_3$  belong to the same signal constellation with  $\mathbf{d}_1 - \hat{\mathbf{d}}_1 = \mathbf{d}_3 - \hat{\mathbf{d}}_3$ , then (15) will reduce to  $d^2((\mathbf{x}_1, \mathbf{x}_3), (\hat{\mathbf{x}}_1, \hat{\mathbf{x}}_3)) = \|\boldsymbol{\eta}_1^T (\mathbf{E}_1 + \mathbf{E}_3)\|^2 + \|\boldsymbol{\eta}_2^T (\mathbf{E}_1 + \mathbf{E}_3)\|^2$ . Following similar steps in the above, we can obtain the PEP expression as

$$P((\mathbf{x}_1, \mathbf{x}_3), (\hat{\mathbf{x}}_1, \hat{\mathbf{x}}_3)) \leq \left(\frac{1}{8N_0}\right)^{-2(L+1)} \left(\prod_{l=0}^L \lambda(l)\right)^{-2}. \quad (20)$$

It is observed from (20) that without rotations the conventional QO-STBC is able to achieve only a diversity order of  $2(L+1)$ .

#### IV. QO-STBCS WITH FULL DECOUPLING

For the quasi-orthogonal structures proposed in [6]–[8] and their rotated versions proposed in [9]–[11], the maximum-likelihood decoding is performed by searching pairs of symbols, i.e., so-called ‘‘pair-decoding,’’ which we have successfully extended to frequency-selective channels in the previous section. Although pair decoding significantly decreases the complexity, this reduction might not be sufficient for frequency-selective channels with long channel memories especially for higher order modulation schemes. In this section, we consider two QO-STBCs which allow full decoupling, i.e., four streams each of which has only one distinct transmitted signal. These codes are defined by

$$\mathbf{A} = \begin{bmatrix} \mathbf{A}_{12} & \mathbf{A}_{34} \\ \mathbf{A}_{12} & -\mathbf{A}_{34} \end{bmatrix} = \begin{pmatrix} x_1 & x_2 & x_3 & x_4 \\ -x_2^* & x_1^* & -x_4^* & x_3^* \\ x_1 & x_2 & -x_3 & -x_4 \\ -x_2^* & x_1^* & x_4^* & -x_3^* \end{pmatrix} \quad (21)$$

$$\hat{\mathbf{A}} = \begin{bmatrix} \mathbf{A}_{12} & \mathbf{0} \\ \mathbf{0} & \mathbf{A}_{34} \end{bmatrix} = \begin{pmatrix} x_1 & x_2 & 0 & 0 \\ -x_2^* & x_1^* & 0 & 0 \\ 0 & 0 & x_3 & x_4 \\ 0 & 0 & -x_4^* & x_3^* \end{pmatrix}. \quad (22)$$

Due to space limitations, we focus our attention on the code defined by (21) in the following, noting that similar analysis holds for (22) as well. The application of (21) to frequency-selective channels requires the implementation of the following encoder rule: ( $k = 1, 4, \dots$ )

$$\begin{aligned} \mathbf{d}_{1,k+1} &= -\mathbf{J}\mathbf{d}_{2,k} & \mathbf{d}_{2,k+1} &= \mathbf{J}\mathbf{d}_{1,k} \\ \mathbf{d}_{1,k+2} &= \mathbf{d}_{1,k} & \mathbf{d}_{2,k+2} &= \mathbf{d}_{2,k} \\ \mathbf{d}_{1,k+3} &= -\mathbf{J}\mathbf{d}_{2,k} & \mathbf{d}_{2,k+3} &= \mathbf{J}\mathbf{d}_{1,k} \\ \mathbf{d}_{3,k+1} &= -\mathbf{J}\mathbf{d}_{4,k} & \mathbf{d}_{4,k+1} &= \mathbf{J}\mathbf{d}_{3,k} \\ \mathbf{d}_{3,k+2} &= -\mathbf{d}_{3,k} & \mathbf{d}_{4,k+2} &= -\mathbf{d}_{4,k} \\ \mathbf{d}_{3,k+3} &= \mathbf{J}\mathbf{d}_{4,k} & \mathbf{d}_{4,k+3} &= -\mathbf{J}\mathbf{d}_{3,k}. \end{aligned}$$

The transmission block format is therefore essentially the same as depicted in Fig. 1, where the encoded data vectors at block indexes  $j = k+2, k+3$ , corresponding to the last two rows in (1), i.e., ( $\mathbf{A}_{34} \ \mathbf{A}_{12}$ ) are replaced now by ( $\mathbf{A}_{12} \ -\mathbf{A}_{34}$ ). Under the assumption that the channel coefficients remain constant over blocks  $k, k+1, k+2$ , and  $k+3$ , the received signals can be written in a matrix form as

$$\underbrace{\begin{bmatrix} \mathbf{r}_k \\ \tilde{\mathbf{r}}_{k+1} \\ \mathbf{r}_{k+2} \\ \tilde{\mathbf{r}}_{k+3} \end{bmatrix}}_{\mathbf{r}} = \underbrace{\begin{bmatrix} \mathbf{H}_1 & \mathbf{H}_2 & \mathbf{H}_3 & \mathbf{H}_4 \\ \mathbf{H}_2^H & -\mathbf{H}_1^H & \mathbf{H}_4^H & -\mathbf{H}_3^H \\ \mathbf{H}_1 & \mathbf{H}_2 & -\mathbf{H}_3 & -\mathbf{H}_4 \\ \mathbf{H}_2^H & -\mathbf{H}_1^H & -\mathbf{H}_4^H & \mathbf{H}_3^H \end{bmatrix}}_{\mathbf{H}} \underbrace{\begin{bmatrix} \mathbf{d}_{1,k} \\ \mathbf{d}_{2,k} \\ \mathbf{d}_{3,k} \\ \mathbf{d}_{4,k} \end{bmatrix}}_{\mathbf{d}} + \underbrace{\begin{bmatrix} \mathbf{n}_k \\ \mathbf{J}\mathbf{n}_{k+1} \\ \mathbf{n}_{k+2} \\ \mathbf{J}\mathbf{n}_{k+3} \end{bmatrix}}_{\mathbf{n}} \quad (23)$$

where we define  $\tilde{\mathbf{r}}_{k+1} = \mathbf{J}\mathbf{r}_{k+1}^*$  and  $\tilde{\mathbf{r}}_{k+3} = \mathbf{J}\mathbf{r}_{k+3}^*$ . Denote  $\tilde{\mathbf{M}}$  as

$$\tilde{\mathbf{M}} = \begin{bmatrix} (\mathbf{H}_\alpha)^{-1/2} & \mathbf{0}_N & \mathbf{0}_N & \mathbf{0}_N \\ \mathbf{0}_N & (\mathbf{H}_\alpha)^{-1/2} & \mathbf{0}_N & \mathbf{0}_N \\ \mathbf{0}_N & \mathbf{0}_N & (\mathbf{H}_\beta)^{-1/2} & \mathbf{0}_N \\ \mathbf{0}_N & \mathbf{0}_N & \mathbf{0}_N & (\mathbf{H}_\beta)^{-1/2} \end{bmatrix} \quad (24)$$

where  $\mathbf{H}_\alpha = |\mathbf{H}_1|^2 + |\mathbf{H}_2|^2$  and  $\mathbf{H}_\beta = |\mathbf{H}_3|^2 + |\mathbf{H}_4|^2$ . Multiplying (23) by  $\tilde{\mathbf{M}}\mathbf{H}^H$  yields

$$\mathbf{r}_{\text{out},k} = 2\mathbf{H}_\alpha^{1/2}\mathbf{d}_{1,k} + \mathbf{n}_{\text{out},k} \quad (25)$$

$$\mathbf{r}_{\text{out},k+1} = 2\mathbf{H}_\alpha^{1/2}\mathbf{d}_{2,k} + \mathbf{n}_{\text{out},k+1} \quad (26)$$

$$\mathbf{r}_{\text{out},k+2} = 2\mathbf{H}_\beta^{1/2}\mathbf{d}_{3,k} + \mathbf{n}_{\text{out},k+2} \quad (27)$$

$$\mathbf{r}_{\text{out},k+3} = 2\mathbf{H}_\beta^{1/2}\mathbf{d}_{4,k} + \mathbf{n}_{\text{out},k+3} \quad (28)$$

where the filtered noise  $\mathbf{n}_{\text{out},j}$  has the variance  $N_0$  per dimension. It should be emphasized that in (25) and (28), each stream consists of a single distinct data vector. Therefore, ML decoding is performed by searching single data vectors. For this code, the MLSE equalizer requires a total number of  $M^{L+1}$  states in trellis implementation which brings a significant reduction in comparison to pair decoding. We should also note that although this code enjoys only a partial diversity with its asymptotical diversity order of 2, it provides a robust performance within the practical SNR range (as elaborated in Section V through simulations) and becomes an attractive solution as a good tradeoff between complexity and performance.

#### V. NUMERICAL RESULTS

In this section, we present Monte Carlo simulation results for the quasi-orthogonal space-time block transmission schemes described

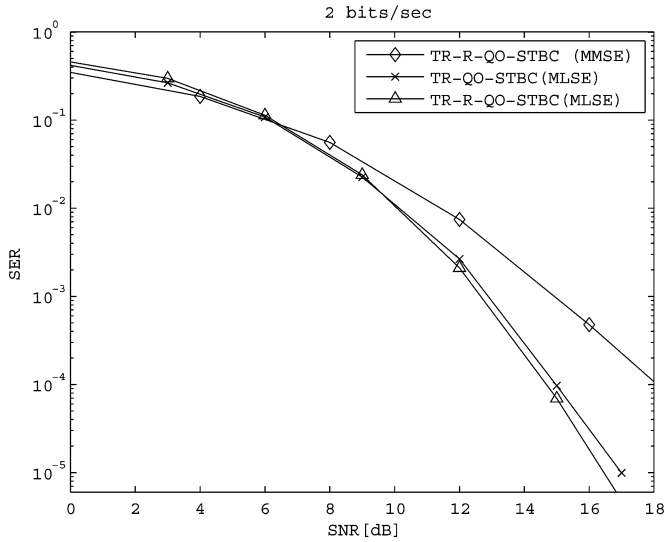


Fig. 2. SER performances of TR-(R)-QO-STBC schemes with MLSE and MMSE equalizers.

and analyzed in this paper. We assume a quasi-static 2-tap frequency-selective Rayleigh-fading channel (i.e., channel memory length  $L = 1$ ) with a uniform delay power profile. In Fig. 2, we present the symbol error rate (SER) performance of the quasi-orthogonal codes with pair decoupling. Specifically, this figure illustrates the effect of constellation phase rotation and performance comparison between MMSE and MLSE implementations. TR implementations of rotated and conventional quasi-orthogonal designs are respectively labeled as TR-R-QO-STBC and TR-QO-STBC. The underlying quasi-orthogonal code for TR-QO-STBC is given by (1) and 4-PSK modulation is assumed. For the rotated version, the quasi-orthogonal code matrix is constructed based on (1), where half of the symbols, i.e., the first two columns of (1), are chosen from 4-PSK signal constellation  $\Theta = \{e^{j((\pi/4)+n(\pi/2))}, n = 0, 1, 2, 3\}$ , and the rest are chosen from the rotated constellation  $e^{j(\pi/4)}\Theta = \{e^{j((\pi/2)+n(\pi/2))}, n = 0, 1, 2, 3\}$ . The rotation angle is chosen as  $\pi/4$  to guarantee full diversity [10]. As predicted by our PEP analysis assuming MLSE receiver (i.e., see (19)), TR-R-QO-STBC yields a diversity order of  $2(L + 1) = 8$  and outperforms TR-QO-STBC in high SNR region which can be observed through the slope of performance curves. It should be further noted that the MLSE equalizer requires the implementation of a  $4^{2(L+1)} = 256$ -state Viterbi algorithm. We have further investigated the MMSE equalizer as an alternative suboptimum lower complexity option. Assuming the rotated quasi-orthogonal code, our simulation results indicate that the diversity order (i.e., predicted by slope of the performance curve in the considered SNR range) is  $\approx 4$ . Specifically, MLSE equalizer outperforms the MMSE equalizer by  $\approx 2.5$  dB at  $SER = 10^{-3}$ .

In Figs. 3 and 4, we compare the performance of the quasi-orthogonal code with full decoupling, i.e., defined by the transmission matrix as in (21),<sup>5</sup> to that with pair decoupling.<sup>6</sup> As benchmarks, we consider two orthogonal STBCs designed for four transmit antennas, i.e., G4 code of [2, Eq. (38)] with rate = 1/2 and the octonion code of

<sup>5</sup>Our Monte Carlo simulation results reveal that codes given by (21) and (22) yield identical performance. Hence, we focus only on one of them, namely (21).

<sup>6</sup>Here, we consider only the rotated version as it is able to provide a better diversity order than the conventional one while still preserving the pair-decoding property.

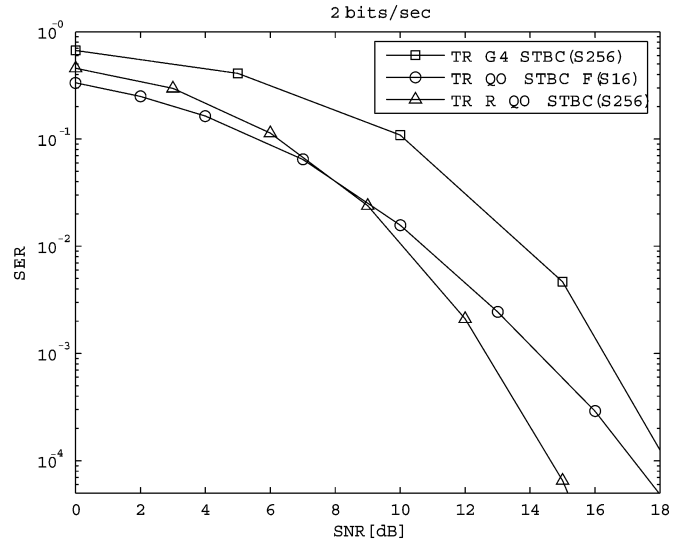


Fig. 3. SER performances of TR-QO-STBC-F, TR-G4-STBC, and TR-R-QO-STBC schemes.

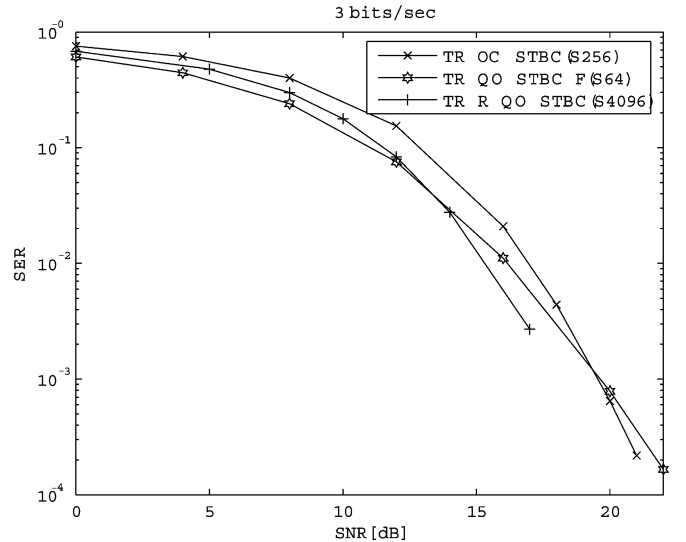


Fig. 4. SER performances of TR-QO-STBC-F, TR-OC-STBC and TR-R-QO-STBC.

[18, Eq. (22)] with rate = 3/4. In Fig. 3, we assume 4-PSK for both full-rate quasi-orthogonal codes under consideration (TR-QO-STBC-F and TR-R-QO-STBC denote the codes with full decoupling and pair decoupling, respectively). To keep the transmission rate fixed, we assume 16-QAM modulation for TR-G4-STBC. The total number of states in MLSE equalizer is  $4^{L+1} = 16$  states for TR-QO-STBC-F,  $4^{2(L+1)} = 256$  states for TR-R-QO-STBC, and  $16^{L+1} = 256$  states for TR-G4-STBC. From the figure, it is clearly observed that both versions of quasi-orthogonal codes outperform the orthogonal G4 for the considered SNR range. Specifically, at  $SER = 10^{-3}$ , we observe performance gains of  $\approx 2-3$  dB over G4 code. Among the considered schemes, TR-QO-STBC-F deserves particular attention with its low complexity. Although it enjoys only a diversity order of 2, it outperforms TR-R-QO-STBC at low SNR values and demonstrates a comparable performance in the medium SNR range. TR-R-QO-STBC with its higher diversity order obviously benefits more from the increasing SNR. Fig. 4 illustrates the SER performance of the above

full-rate quasi-orthogonal codes with 8-PSK providing a transmission rate of 3 b/s. The benchmarking orthogonal code for this case is the octonion code of [18] with rate =  $3/4$  and 16-QAM modulation (labeled as TR-OC-STBC). The total number of states in MLSE equalizer is  $8^{(L+1)} = 64$  states for TR-QO-STBC-F,  $8^{2(L+1)} = 4096$  states for TR-R-QO-STBC, and  $16^{(L+1)} = 256$  states for TR-OC-STBC. It is observed from our simulation study that TR-R-QO-STBC outperforms TR-OC-STBC in the whole SNR range although their diversity order is the same. The main disadvantage of TR-R-QO-STBC for this scenario is its associated complexity.<sup>7</sup> For this particular case, TR-QO-STBC-F with 64-state MLSE equalizer seems to be even more attractive as it has the lowest complexity among the three schemes. It is even able to outperform its competitor TR-OC-STBC (with 256-state MLSE equalizer) for a wide range of SNR values (up to 20 dB) which can be considered practical for most purposes.

## VI. CONCLUSION

We have investigated time-domain equalization for QO-STBC, carefully exploiting the inherent quasi-orthogonality to design low-complexity receivers. The proposed scheme extends QO-STBCs to frequency-selective channels by imposing the quasi-orthogonal structure at a block-level instead of the symbol-level realization for the flat-fading channel case. Our designs guarantee that the “pair-decoding” property of QO-STBC is preserved in the presence of frequency-selectivity yielding low-complexity receivers. In addition, we investigated QO-STBC schemes which allow full decoupling and provide further reductions in complexity at the receiver. We have demonstrated through the derivation of PEP expressions that our schemes are able to achieve a maximum diversity order of  $2(L + 1)$  for conventional QO-STBC and  $4(L + 1)$  for rotated QO-STBC over frequency-selective channels with a channel memory of  $L$ . Extensive Monte Carlo simulations were conducted to confirm the analytical observations and to further provide a comprehensive performance comparison among the competing schemes. The application of frequency-domain single-carrier equalization to quasi-orthogonal codes can be also found in [14] where similar observations on the achievable diversity order are reported.

## REFERENCES

- [1] V. Tarokh, N. Seshadri, and A. R. Calderbank, “Space time codes for high data rate wireless communications: Performance criterion and code construction,” *IEEE Trans. Inf. Theory*, vol. 44, pp. 722–765, Mar. 1998.
- [2] V. Tarokh, H. Jafarkhani, and A. R. Calderbank, “Space time block codes from orthogonal design,” *IEEE Inf. Theory*, vol. 45, pp. 1456–1466, Jul. 1999.
- [3] S. M. Alamouti, “A simple transmitter diversity scheme for wireless communications,” *IEEE J. Sel. Areas Commun.*, pp. 1451–1458, Oct. 1998.
- [4] W. Su and X.-G. Xia, “On space-time block codes from complex orthogonal designs,” *Wireless Personal Commun.*, vol. 25, no. 1, pp. 1–26, Apr. 2003.
- [5] H. Wang and X.-G. Xia, “Upper bounds of rates of complex orthogonal space-time block codes,” *IEEE Trans. Inf. Theory*, vol. 49, pp. 2788–2796, Oct. 2003.
- [6] H. Jafarkhani, “A quasi-orthogonal space-time block code,” *IEEE Trans. Commun.*, vol. 49, pp. 1–4, Jan. 2001.
- [7] C. B. Papadias and G. J. Foschini, “Capacity-approaching space-time codes for systems employing four transmitter antennas,” *IEEE Trans. Inf. Theory*, vol. 49, pp. 726–732, Mar. 2003.
- [8] O. Tirkkonen, A. Boariu, and A. Hottinen, “Minimal nonorthogonality rate 1 space-time block code for 3+ TX antennas,” in *Proc. IEEE 6th Int. Symp. Spread-Spectrum Techniques Applications (ISSSTA 2000)*, Sep. 2000, pp. 429–432.
- [9] W. Su and X.-G. Xia, “Signal constellations for quasi-orthogonal space-time block codes with full diversity,” *IEEE Trans. Inf. Theory*, vol. 50, pp. 2331–2347, Oct. 2004.
- [10] D. Wang and X.-G. Xia, “Optimal diversity product rotations for quasi-orthogonal STBC with MPSK,” *IEEE Commun. Lett.*, vol. 9, May 2005.
- [11] N. Sharma and C. Papadias, “Full-rate full-diversity linear quasi-orthogonal space-time codes for any number of transmit antennas,” *EURASIP J. Appl. Signal Process.*, pp. 1246–1256, Sep. 2004.
- [12] N. Al-Dhahir, “Overview and comparison of equalization schemes for space time coded signals with application to EDGE,” *IEEE Trans. Signal Process.*, vol. 50, no. 10, pp. 2477–2488, Oct. 2002.
- [13] E. Lindskog and A. Paulraj, “A transmit diversity scheme for channel with ISI,” in *Proc. Int. Conf. Communication*, Jun. 2000, pp. 307–311.
- [14] H. Mheidat, M. Uysal, and N. Al-Dhahir, “Time-and frequency-domain equalization for quasi-orthogonal STBC over frequency-selective channels,” in *Proc. IEEE Int. Conf. Communications (ICC)*, Paris, France, Jun. 2004.
- [15] S. Zhou and G. B. Giannakis, “Single-carrier space-time block coded transmissions over frequency-selective fading channels,” *IEEE Trans. Inf. Theory*, vol. 49, no. 1, pp. 164–179, Jan. 2003.
- [16] G. E. Bottomley and S. Chennakeshu, “Unification of MLSE receivers and extension to time-varying channels,” *IEEE Trans. Commun.*, vol. 46, pp. 464–472, Apr. 1998.
- [17] E. Larson and P. Stoica, *Space-Time Block Coding for Wireless Communications*. Cambridge, U.K.: Cambridge Univ. Press, 2003.
- [18] O. Tirkkonen and A. Hottinen, “Square-matrix embeddable space-time block codes for complex signal constellations,” *IEEE Trans. Inf. Theory*, vol. 48, pp. 384–395, Feb. 2002.

<sup>7</sup>Due to the long simulation time involved with Viterbi algorithm implementation of 4096 states, we only included simulation results up to  $SER = 10^{-3}$ .